Over-The-Air Testing for Carrier Aggregation Enabled MIMO Terminals Using Radiated Two-Stage Method

Gao, Huaqiang; Wang, Weiming; Fan, Wei; Wu, Yongle ; Liu, Yuanan; Pedersen, Gert F.

Published in:
IEEE Access

DOI (link to publication from Publisher):
10.1109/ACCESS.2018.2881046

Publication date:
2018

Document Version
Publisher's PDF, also known as Version of record

IEEE Access
Multidisciplinary | Rapid Review | Open Access Journal

Received October 2, 2018, accepted November 8, 2018, date of publication November 12, 2018,
date of current version December 18, 2018.

Digital Object Identifier 10.1109/ACCESS.2018.2881046

Over-the-Air Testing for Carrier Aggregation Enabled MIMO Terminals Using Radiated Two-Stage Method

HUAQIANG GAO[1], WEIMIN WANG[1], WEI FAN[2], YONGLE WU[1], YUANAN LIU[1], AND GERT FRØLUND PEDERSEN[2]

[1]Beijing Key Laboratory of Work Safety Intelligent Monitoring, Department of Electronic Engineering, Beijing University of Posts and Telecommunications, 100876 Beijing, China
[2]Department of Electronic Systems, Faculty of Engineering and Science, Antenna Propagation and Millimeter-Wave Systems Section, Aalborg University, 9220 Aalborg, Denmark

Corresponding author: Weimin Wang (wangwm@bupt.edu.cn)

This work was supported by the National Natural Science Foundation of China under Grant 61701041, Grant 61671084, and Grant 61821001.

ABSTRACT Multiple-input multiple-output (MIMO) over-the-air (OTA) testing of wireless devices has become increasingly attractive in radiated performance evaluation. As one of the OTA testing methods, the radiated two-stage (RTS) method achieves flexible channel models with low-system cost. However, the existing MIMO OTA testing using RTS method is valid only for single carrier frequency application. This paper applies the RTS method to multiple carrier frequency applications [carrier aggregation (CA)]. Two setups are presented to discuss system cost and calibration time. To validate the RTS OTA testing for CA, the transfer matrices from the OTA antenna ports to device under test antenna ports in three types of RF shielded enclosure are investigated. The results demonstrate that the applied RTS method for CA works better in anechoic chambers. One calibration matrix might need to be adopted for each component carrier when the frequency separation of component carriers is large.

INDEX TERMS Multiple-input multiple-output (MIMO), over-the-air (OTA) testing, radiated two-stage (RTS) method, carrier aggregation (CA), anechoic chamber, chamber loading.

I. INTRODUCTION

With the rapid development of wireless communication systems, multiple-input multiple-output (MIMO) technology has been introduced in Long Term Evolution (LTE) networks to increase the data rate of wireless devices [1]. The carrier aggregation (CA) introduced in LTE-Advanced achieves higher data rate [2]–[4], which is also expected to be employed in fifth-generation (5G) wireless systems [5], [6]. CA simultaneously using multiple carriers aggregates multiple frequency bands to increase transmission bandwidth effectively. As shown in Fig. 1, there are three ways in which LTE carriers are aggregated. Each component carrier might have a bandwidth of 1.4, 3, 5, 10, 15, or 20 MHz [7]. However, CA increases the complexity of device realization [8]. The realization of the transceiver front-end supporting multiple band combinations is one of the key challenges in the process of product development. In order to verify the transceiver front-end realization, the device performance needs to be evaluated following the device realization.

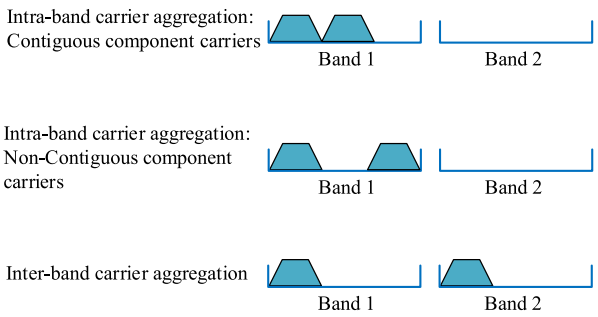

FIGURE 1. Three ways for carrier aggregation.

Over-the-air (OTA) testing of MIMO devices performance has attracted growing attention from both academia and industry recently [9], [10]. Thus, it is essential for the CA enabled MIMO devices to be tested over the air and verified before the final rollout. Three OTA testing methodologies have been presented in the literature, namely

the multi-probe anechoic chamber (MPAC) based method [11]–[15], the reverberation chamber (RC) based method [16]–[19], and the radiated two-stage (RTS) method (also known as the wireless cable method) [20]–[36]. In MPAC methods and RC methods, the target propagation channel is emulated to evaluate the complete end-to-end performance of the device under test (DUT). A suitable test area where DUT would experience the realistic channel is produced in an anechoic chamber using multiple probe antennas each connected to one RF output port of channel emulator (CE) in MPAC methods [12]. In RC methods, rich multipath environment is produced in the reverberation chamber by mechanical stirrers rotation and metallic wall reflection [17], [19]. Thus the DUT antenna pattern is directly included in both MPAC and RC methods testing. The difference between MPAC methods and RC methods lies in the control on the reproduced channels. The former emulates arbitrary spatial channel models theoretically, whereas the latter generates isotropic spatial channels with Rayleigh fading [37]. On the other hand, arbitrary channel models are implemented also using the RTS method due to the use of CEs. Unlike the MPAC method and the RC method, the RTS method guides the specified test signals to the DUT antenna ports over the air [21]. The principle is to compensate the transfer matrix between the OTA antenna ports and DUT antenna ports using a calibration matrix implemented in CEs. However, the DUT antenna pattern is indirectly included during the test because of the pattern measurement in the first stage and its embedding in the CE in the second stage. Therefore, the RTS method is effective only on condition that the DUT antenna patterns are static and not adaptive [30].

The RTS method has advantage over MPAC methods since it requires much less number of OTA antennas. The former is highly attractive especially for the large DUT equipped with limited number of antennas [35]. This is because that the same number of required OTA antennas as the DUT receive antennas is employed for the RTS method to achieve the ''wireless cable'' transmission, independent of the channel models and DUT size. Furthermore, less number of required OTA antennas reduce the system cost since the required number of RF interface channels in the CE depends directly on the number of OTA antennas. Several efforts have been devoted to the RTS method [20]–[36], which can be basically divided into three categories, namely calibration matrix determination [21], [30], [32], [35], measurement error analysis [26], [28], [31], [36], and method application [20], [22], [25], [27]. However, the applied RTS method mentioned above is only valid for single carrier. As discussed earlier, it is essential and promising to perform OTA testing of CA enabled MIMO terminals. Limited contributions have reported this issue. Among the three OTA testing methods, the RC method has been reported for CA testing in the literature [38]–[40], and the MPAC method for CA is applied in commercial applications. To the best of our knowledge, no work has been reported on MIMO OTA testing using the RTS method for the CA with multiple carriers.

In this paper, MIMO OTA testing for CA using the RTS method is investigated. The main contributions of this paper are summarized as below:

1) Two setups are proposed to apply the RTS method to the OTA testing of CA with multiple carriers where wireless cable connections are established for each component carrier.
2) The transfer matrices in three types of RF shielded enclosure are measured to verify the feasibility of RTS method in these RF shielded enclosure when one calibration matrix is employed for single carrier.
3) The applied RTS method for CA is validated in anechoic chambers using one calibration matrix for each component carrier.

The paper is organized as follows. In Section II, the RTS testing method for single carrier is reviewed and its shortage is presented for multiple carriers. In Section III, two setups are presented to apply RTS testing method to CA, in which system cost and calibration time are discussed. In Section IV, measurement validation is performed for RTS testing of CA. Conclusion is given in Section V.

II. PROBLEM FORMULATION

The time-variant channel frequency response (CFR) $\boldsymbol{H}(f,t) = \{h_{n,m}(f,t)\} \in \mathbb{C}^{N\times M}$ is given for a MIMO system equipped with M base station (BS) antennas and N user equipment (UE) antennas, in which $h_{n,m}(f,t)$ repesents the CFR from the mth BS antenna port to the nth UE antenna port. Therefore, $\boldsymbol{H}(f,t)$ includes the effects of the BS antenna pattern, propagation channel, and the UE antenna pattern. The MIMO signal model is expressed as [30]:

$$\boldsymbol{y}(f,t) = \boldsymbol{H}(f,t)\boldsymbol{x}(f,t) + \boldsymbol{n}(f,t) \tag{1}$$

where $\boldsymbol{y}(f,t) \in \mathbb{C}^{N\times 1}$, $\boldsymbol{x}(f,t) \in \mathbb{C}^{M\times 1}$, and $\boldsymbol{n}(f,t) \in \mathbb{C}^{N\times 1}$ denote the receive signal vector at the N UE antenna ports, the transmit signal vector at the M BS antenna ports, and the noise vector at the N UE antenna ports, respectively. For the sake of simplicity, noise vector $\boldsymbol{n}(f,t)$ is ignored in the study. Specifically, we take 2×2 MIMO (i.e. $M = N = 2$) as an example in the following discussion.

Compared with the conducted two-stage (CTS) OTA testing method [41], [42], the RTS method achieves the functionality of CTS cable connections without actual RF cable connections. The first stage of RTS method is the same as that of CTS method where DUT antenna pattern measurement is performed. The second stage is to achieve the calibration matrix and perform the MIMO throughput test. A brief illustration of the RTS method in the second stage is shown in Fig. 2. $\boldsymbol{A} = \{a_{ij}\} \in \mathbb{C}^{2\times 2}$ denotes the transfer matrix between the OTA antenna ports and DUT antenna ports where a_{ij} stands for the complex transmission coefficient from OTA antenna port j to DUT antenna port i $(i, j \in [1, 2])$. Therefore, it includes the effects of OTA antennas, multipath propagation inside the RF shielded enclosure, and DUT antennas. The specified testing signals guided to the DUT antenna ports are

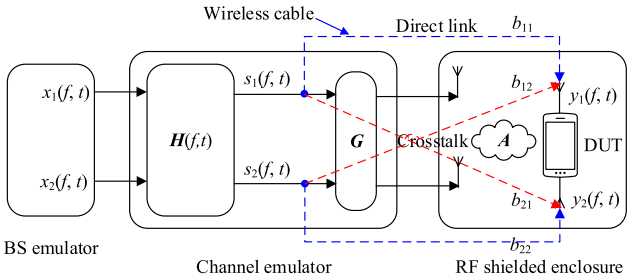

FIGURE 2. A brief illustration of the second stage in the RTS method.

as follow [35]:

$$\begin{aligned} \boldsymbol{y}(f,t) &= \boldsymbol{AGH}(f,t)\boldsymbol{x}(f,t) \\ &= \boldsymbol{AGs}(f,t) \\ &= \boldsymbol{s}(f,t) \end{aligned} \tag{2}$$

where $\boldsymbol{H}(f,t)$ is the target channel model including the DUT antenna patterns. $\boldsymbol{x}(f,t)$ is the transmit signals at the BS emulator output ports. $\boldsymbol{s}(f,t)$ is the target test signals to DUT antenna ports.

The key of RTS method in the second stage is to establish wireless cable connections. Two wireless cable connections are established because of two receive antennas on DUT. In order to achieve the two wireless cable connections, we need to set calibration matrix $\boldsymbol{G} \in \mathbb{C}^{2\times 2}$ in the CE so that the following is approximated.

$$\boldsymbol{AG} = \begin{bmatrix} b_{11} & b_{12} \\ b_{21} & b_{22} \end{bmatrix} = \begin{bmatrix} 1 & 0 \\ 0 & 1 \end{bmatrix} \tag{3}$$

To evaluate the approximation, the isolation levels between the desired direct link and undesired crosstalk are examined. The isolation levels for the two wireless cable connections are defined as

$$I_1 = \frac{|b_{11}|}{|b_{21}|} \tag{4}$$

$$I_2 = \frac{|b_{22}|}{|b_{12}|} \tag{5}$$

As mentioned before, there are several solutions to determine $\boldsymbol{G}$ and $\boldsymbol{A}$ in contributions [21], [25], [30], [32], [35], where the pair of $\boldsymbol{G}$ and $\boldsymbol{A}$ is only valid for single carrier. However, $\boldsymbol{A}$ might vary as the carrier changes in the case of multiple carriers. If $\boldsymbol{G}$ remains unchanged, $\boldsymbol{A}_c\boldsymbol{G} = \begin{bmatrix} 1 & 0 \\ 0 & 1 \end{bmatrix}$ would not be approximated for all carriers ($\boldsymbol{A}_c$ denotes the transfer matrix for different carriers). Therefore, $\boldsymbol{G}$ might need to be updated according to different carriers. The MIMO signal model is rewritten for CA as:

$$\begin{aligned} \boldsymbol{y}(f,t) &= \sum_{c=1}^{C} \boldsymbol{A}_c\boldsymbol{G}_c\boldsymbol{H}_c(f,t)\boldsymbol{x}_c(f,t) \\ &= \sum_{c=1}^{C} \boldsymbol{A}_c\boldsymbol{G}_c\boldsymbol{s}_c(f,t) \end{aligned} \tag{6}$$

where c and C stands for component carrier index and the number of component carriers, respectively. $\boldsymbol{A}_c$ and $\boldsymbol{G}_c$ denote the transfer matrix and the calibration matrix for component carrier c, respectively. $\boldsymbol{s}_c$ denotes the target test signals for component carrier c.

III. RTS METHOD FOR CA

In this part, we propose the first approach to conducting RTS OTA testing for CA where two setups are presented. The focus is on the second stage of RTS method where wireless cable connections are established for CA. Fig. 3 illustrates the two setups (Setup A and B) to perform the OTA testing for CA using RTS method in the second stage where two component carriers are employed as an example. The principle can be directly applied to multiple component carriers.

Setup A is a straightforward approach that is to directly employ multiple sets of setup resources under the circumstances of single carrier according to the number of component carriers, as shown in Fig. 3(a). Two MIMO streams $x_{1,C1}(f,t)$ and $x_{2,C1}(f,t)$ of component carrier 1 generated from BS emulator are connected to two RF input ports of CE, respectively. The channel model $\boldsymbol{H}_{C1}(f,t)$ of component carrier 1 is generated in digital baseband of CE. Then the calibration matrix $\boldsymbol{G}_{C1}$ is determined and implemented in RF band of CE for component carrier 1. Finally, two RF output ports of CE are connected to two OTA antenna ports, respectively. The configuration is the same for component carrier 2 using another set of setup resources. Four OTA antennas and the DUT are placed in the same RF shielded enclosure. For each component carrier regardless of how they are aggregated (as shown in Fig. 1), the determination process of $\boldsymbol{G}_c$ is performed respectively just as it is done in the case of single carrier. Two cases of determining $\boldsymbol{G}_c$ are discussed. In the first case, $\boldsymbol{G}_c$ is determined on the basis of reference signal received power (RSRP) or received signal amplitude and relative phase (RSARP) value per DUT antenna port reported by DUT [30]–[36]. Only one $\boldsymbol{G}_c$ is obtained for each component carrier since there is one RSRP or RSARP value over the whole LTE band. In the second case, $\boldsymbol{G}_c$ is determined by inverting $\boldsymbol{A}_c$ obtained in several ways, namely estimation [35], calculation [20]–[24], [26]–[29], and direct measurement [25]. One $\boldsymbol{A}_c$ needs to be obtained for each component carrier because only one $\boldsymbol{G}_c$ can be applied in the RF band of CE. Then the determined $\boldsymbol{G}_c$ for each component carrier is implemented separately in the RF band of CE to perform subsequent throughput testing.

In the second case of determining $\boldsymbol{G}_c$, Setup B is presented to save system cost (including CE hardware resources and the number of OTA antennas) and calibration time, as shown in Fig. 3(b). In this case, the determined $\boldsymbol{G}_c$ are directly applied to the target channel model for each component carrier in the digital baseband of CE. In Setup B, BS emulator generates MIMO signals $x_{1,C1}(f,t)$, $x_{2,C1}(f,t)$, $x_{1,C2}(f,t)$ and $x_{2,C2}(f,t)$ of two component carriers separately to four RF input ports of CE. The generated channel model $\boldsymbol{H}_{C1}(f,t)$ and the determined calibration matrix $\boldsymbol{G}_{C1}$ are combined

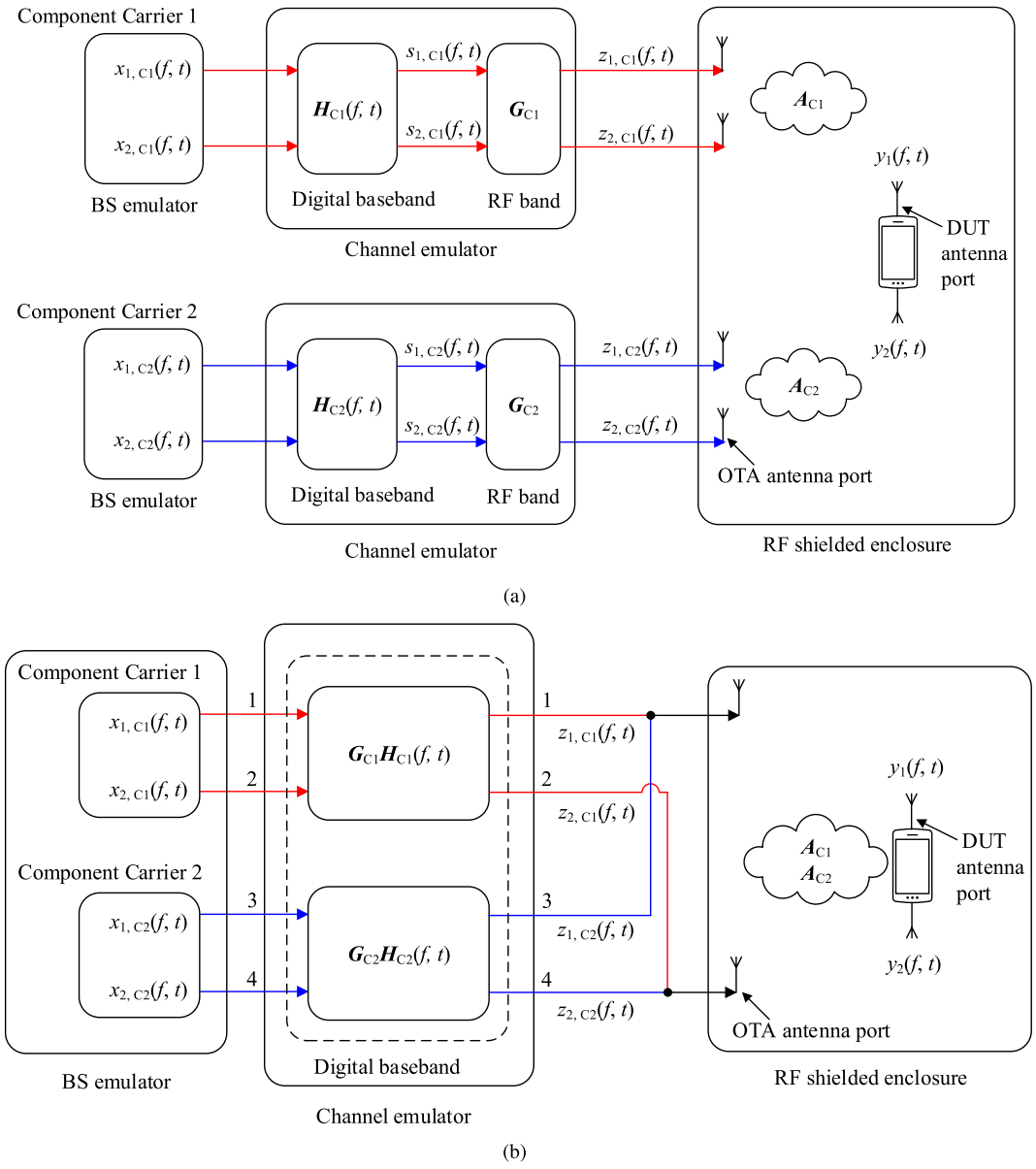

FIGURE 3. Two setups to conduct RTS OTA testing for CA with two component carriers as an example, namely (a) Setup A, and (b) Setup B. $x_{1,C1}(f,t)$ and $x_{2,C1}(f,t)$ are two MIMO streams of component carrier 1 from BS emulator, whereas $x_{1,C2}(f,t)$ and $x_{2,C2}(f,t)$ are two MIMO streams of component carrier 2 from BS emulator. $H_{C1}(f,t)$ and $H_{C2}(f,t)$ are the channel models for component carrier 1 and component carrier 2, respectively. G_{C1} and G_{C2} are the calibration matrices for component carrier 1 and component carrier 2, respectively. $s_{1,C1}(f,t)$ and $s_{2,C1}(f,t)$ are two target MIMO streams of component carrier 1 to DUT antenna ports, whereas $s_{1,C2}(f,t)$ and $s_{2,C2}(f,t)$ are two target MIMO streams of component carrier 2 to DUT antenna ports. A_{C1} and A_{C2} are the transfer matrices for component carrier 1 and component carrier 2, respectively. $z_{1,C1}(f,t)$ and $z_{2,C1}(f,t)$ are two MIMO streams of component carrier 1 at RF output ports of the CE, whereas $z_{1,C2}(f,t)$ and $z_{2,C2}(f,t)$ are two MIMO streams of component carrier 2 at RF output ports of the CE. $y_1(f,t)$ and $y_2(f,t)$ are two MIMO streams of two combined component carriers received at DUT antenna port.

in the digital baseband of CE for component carrier 1. Simultaneously, the generated $\boldsymbol{H}_{C2}(f,t)$ and the determined $\boldsymbol{G}_{C2}$ are combined in the digital baseband of CE for component carrier 2. Finally in the RF output ports of CE, the same MIMO streams ($z_{1,C1}(f,t)$ and $z_{1,C2}(f,t)$, $z_{2,C1}(f,t)$ and $z_{2,C2}(f,t)$) of two component carriers are combined to be transmitted through one OTA antenna to the corresponding DUT antenna port. Two OTA antennas are located in the RF shielded enclosure. In Setup A, two different OTA antennas are employed for each component carrier. Thus, after obtaining the transfer matrix $\boldsymbol{A}_{C1}$ for component carrier 1, we also need to activate another two OTA antennas to obtain $\boldsymbol{A}_{C2}$ for component carrier 2. However, two same OTA antenna are used to obtain $\boldsymbol{A}_{C1}$ and $\boldsymbol{A}_{C2}$ at two carrier frequencies for two component carriers in Setup B, respectively. Therefore, it is more time-saving to determine

$\boldsymbol{A}_c$ and $\boldsymbol{G}_c$ in Setup B. Note that it requires that the frequency band of two OTA antennas of each component carrier covers the corresponding component carrier in Setup A, whereas it requires that the frequency band of two OTA antennas covers two component carriers in Setup B.

IV. MEASUREMENT VALIDATION

In this part, the measurement validation is conducted for the OTA testing of CA using the RTS method. Note that any method to obtain $\boldsymbol{A}_c$ and $\boldsymbol{G}_c$ in the literature can be used. Specifically, the direct measurement of $\boldsymbol{A}_c$ and $\boldsymbol{G}_c$ inverting $\boldsymbol{A}_c$ are selected as an example to validate the RTS method for CA, which is applicable to each setup in Fig. 3. In addition, the mockup antennas with accessible antenna connectors are used for the measurement of the transfer matrix.

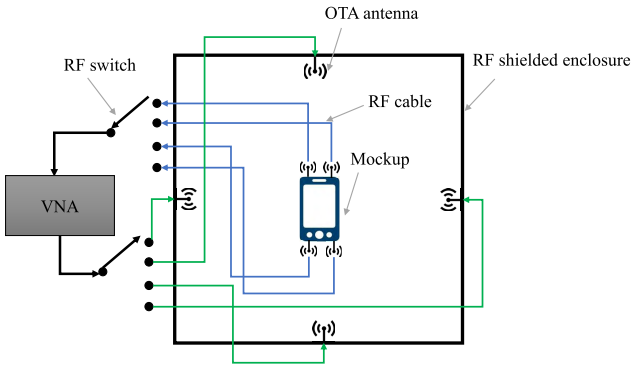

FIGURE 4. An illustration of the measurement system.

A. MEASUREMENT SYSTEM AND SETUP

The measurement system is shown in Fig. 4. It consists of a two-port vector network analyzer (VNA), two single pole quad throw switches, a RF shielded enclosure, four OTA antennas, and a mockup equipped with four antennas. There are three types of RF shielded enclosure investigated here, namely the reverberation chamber without absorber (named Scenario A in the following), the reverberation chamber loaded with absorber (named Scenario B in the following), and the anechoic chamber (named Scenario C in the following). The measurement setup is detailed in Table 1.

The transfer matrices in three types of RF shielded enclosure are measured, via recording the frequency responses of 16 transmission coefficients (i.e. from four OTA antennas to four antennas on the mockup) with the VNA, together with two RF switches. As a result, a 4×4 transfer matrix is obtained first. Then the 2×2 transfer matrix $\boldsymbol{A}(f)$ is selected from the 4×4 transfer matrix in order to investigate the 2×2 MIMO system. Noted that the measured frequency band is selected in 5.1 GHz~5.8 GHz as an example due to the frequency band of OTA antennas. Although the measured frequency band does not contain the current LTE and 5G bands, the principle can be directly applied to these bands.

TABLE 1. Setup and specifications of each component in the measurement system.

Component	Setup and specifications
VNA	The frequency sweep was recorded from 5.1 GHz to 5.8 GHz with 1001 frequency samples for Scenario A and Scenario B, and with 2241 frequency samples for Scenario C. Intermediate frequency (IF) in the VNA was set to 1 KHz.
OTA antenna	Linear polarized directional antennas with frequency band from 5.15 GHz to 5.875 GHz and the product type is SPA-5600/40/14/0/V. The OTA antennas are placed on the four sides of the wall for Scenario A and B, and placed on the four vertices of a square (each side around 1 m) for Scenario C, as shown in Fig. 5.
RF shielded enclosure	Three types of RF shielded enclosure are considered, as shown in Fig. 5. Scenario A: A metallic box of size 42cm $\times$ 42cm $\times$ 42cm without absorbers; Scenario B: A metallic box of size 42cm $\times$ 42cm $\times$ 42cm loaded with absorbers; Scenario C: Anechoic chamber.
Mock-up	The mockup with four wideband monopole antenna elements was designed, as shown in Fig. 6. The mockup operates at around 5.5 GHz. The mockup was placed on a polystyrene support with 45° tilted.

B. MEASUREMENT RESULTS

In the throughput measurements using the RTS method, wireless cable connections are established already well with an isolation level of 18 dB [20]. Therefore, an isolation level of 18 dB is used here as the standard to judge whether a good wireless cable connection is already established. Note that the isolation levels above 18 dB are recorded as 18 dB in the following results of isolation levels.

In this part, the transfer matrix in three scenarios are investigated first. Then we validate the feasibility of RTS method adopting one calibration matrix for single carrier in three scenarios. Next, the validity of OTA testing for CA using RTS method is illustrated in anechoic chambers. Finally, the isolation levels degradation among different component carriers adopting one calibration matrix is discussed in anechoic chambers.

1) TRANSFER MATRIX

The measured CFR and channel impulse response (CIR) from one OTA antenna port to one mockup antenna port in the three scenarios are shown in Fig. 7. The CIR is obtained by an inverse Fourier transform of CFR. Based on the measured CIR, we calculated the root mean square (rms) delay spread within a dynamic range of 40 dB to measure the multipath richness in the three scenarios. Less multipath exists with smaller delay spread. The delay spread is 72.1 ns, 4.2 ns, and 1.9 ns in Scenario A, B, and C, respectively. Therefore, rich multi-paths exist in Scenario A, whereas there is basically no multi-path existing in Scenario C. Much fewer multi-paths exist in Scenario B compared with Scenario A. It also explains that the CFR in Scenario A is frequency

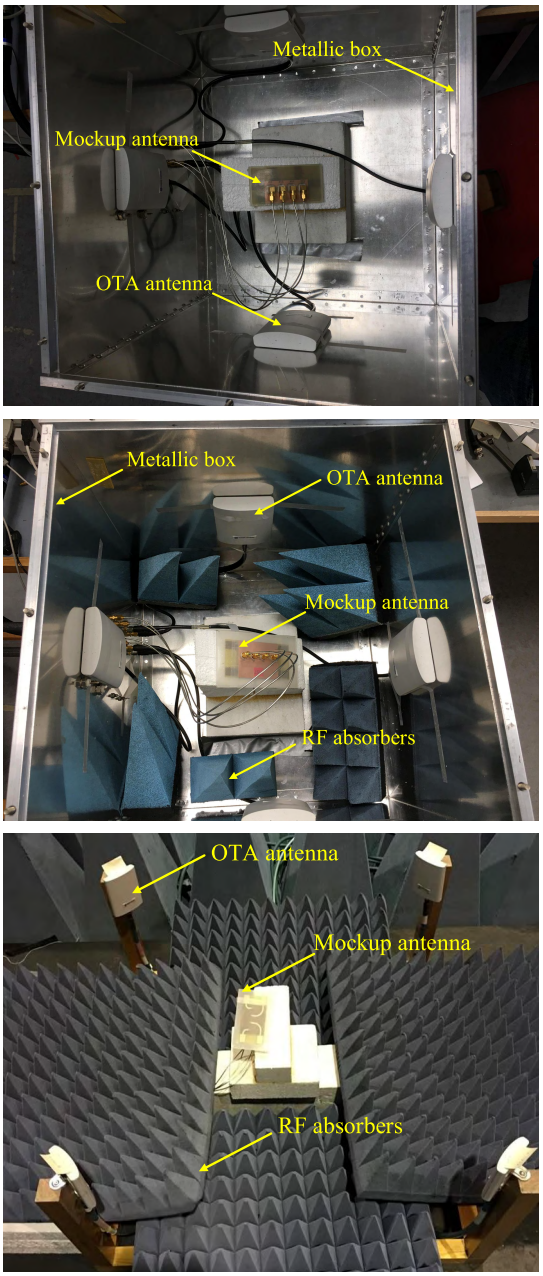

FIGURE 5. The measurement setup in three types of RF shielded enclosure, namely Scenario A (top), Scenario B (middle), and Scenario C (bottom).

selective, whereas it is frequency flat in Scenario C. Much less frequency-selective CFR is presented in Scenario B compared with Scenario A. Comparing Scenario A and B, the absorber loaded in the reverberation chamber greatly reduces the multipath effects, as expected.

2) ONE CALIBRATION MATRIX FOR SINGLE CARRIER

As mentioned before, only one calibration matrix determined via RSRP or RSARP value is obtained for single carrier because there is only one reported RSRP or RSARP value over the whole LTE band [30], [32], [35]. Therefore, in order

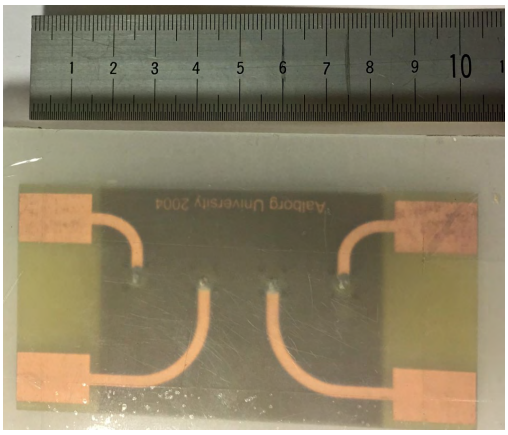

FIGURE 6. The mockup applied in the measurement.

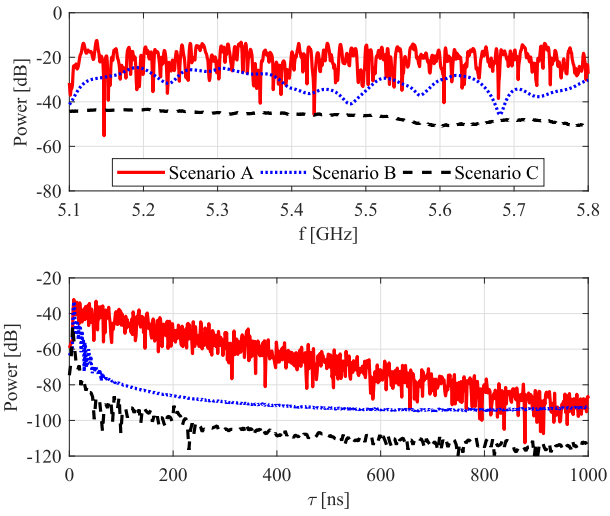

FIGURE 7. The measured CFR (top) and CIR (below) between from one OTA antenna port to one mockup antenna port in three scenarios.

to verify whether one calibration matrix achieves wireless cable connections for single carrier, the isolation levels over the frequency band are investigated where one calibration matrix determined by center frequency is adopted as an example.

TABLE 2. Parameter setting for single carrier in three scenarios.

RF shielded enclosure	Component carrier (Index)	Frequency band (GHz)	Center frequency (GHz)	Frequency samples (Number)
Scenario A and B	1	5.4500∼5.4696	5.4598	29
Scenario C	2	5.4500∼5.4700	5.4600	65

The single carrier setting in three scenarios is detailed in Table 2. Fig. 8 shows the isolation levels of two connections over the whole band using one calibration matrix in the three scenarios. There are isolation levels smaller than 18 dB existing over the frequency band in both Scenario A and B, whereas Scenario C keeps good isolation levels over the

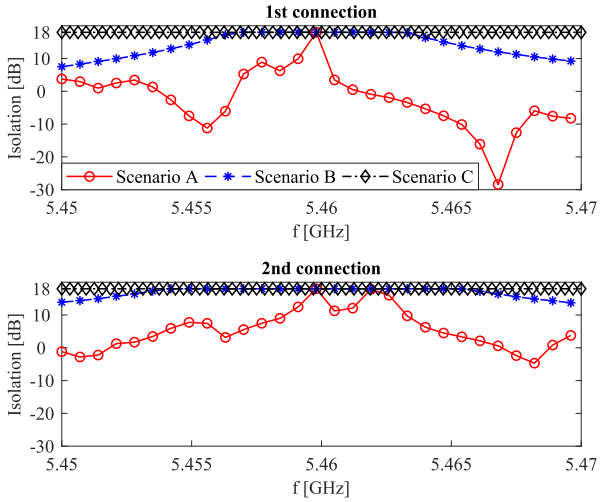

FIGURE 8. Isolation levels of two connections over the single band using one calibration matrix in three scenarios.

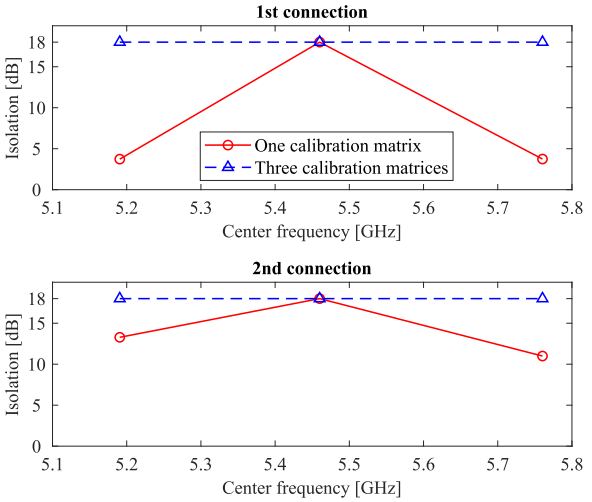

FIGURE 9. Isolation levels of two connections at the center frequencies of three component carriers in Scenario C adopting the calibration matrix determined by component carrier 2 and adopting one calibration matrix per component carrier, respectively.

frequency band. It shows that wireless cable connections are established better in anechoic chambers when one calibration matrix is employed for single carrier. In addition, a small RF shielded anechoic box presented in [30] can be applied instead of anechoic chamber in RTS testing to greatly reduce system cost.

TABLE 3. Parameter setting for three component carriers in Scenario C.

RF shielded enclosure	Component carrier (Index)	Frequency band (GHz)	Center frequency (GHz)	Frequency samples (Number)
Scenario C	2	5.4500∼5.4700	5.4600	65
	3	5.1806∼5.2006	5.1906	65
	4	5.7503∼5.7703	5.7603	65

3) CA VALIDATION

To demonstrate the validation of RTS OTA testing for CA, the isolation level results for multiple carriers adopting one and multiple calibration matrices are compared. The CA with three component carriers are considered here as an example. The detailed setting of component carriers in Scenario C is tabulated in Table 3. Fig. 9 shows the isolation levels of two connections at the center frequencies of three component carriers in Scenario C adopting the calibration matrix determined by component carrier 2 and adopting one calibration matrix per component carrier, respectively. The good isolation levels are achieved only for carrier 2 when the calibration matrix determined by component carrier 2 is employed. When one calibration matrix per component carrier is adopted, good isolation levels are achieved for each carrier. It indicates that wireless cable connections of RTS method are established well for CA.

4) DISCUSSION

Comparing the isolation level results adopting one calibration matrix in anechoic chambers from Fig. 8 and Fig. 9,

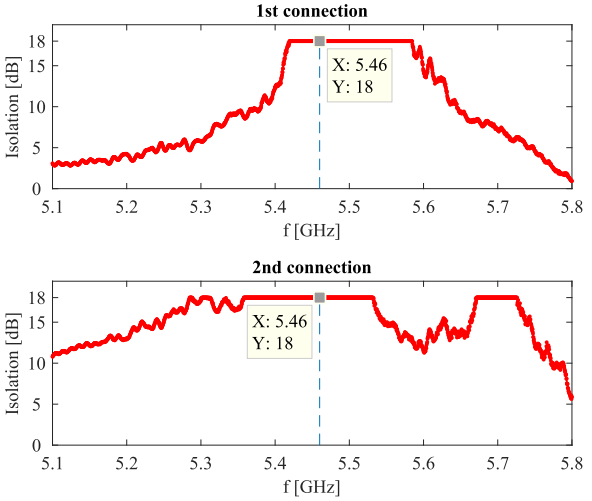

FIGURE 10. Isolation levels of two connections over a frequency band from 5.1 GHz to 5.8 GHz adopting one calibration matrix determined at 5.46 GHz in Scenario C.

isolation levels keep good in one component carrier while they degrade for other component carriers. In order to interpret the isolation levels degradation among different component carriers adopting one calibration matrix in anechoic chambers, Fig. 10 presents the isolation levels over a frequency band from 5.1 GHz to 5.8 GHz adopting one calibration matrix determined at 5.46 GHz in Scenario C. It can be seen that isolation levels keep good when frequency is in the vicinity of 5.46 GHz, whereas they start to degrade for frequency far from 5.46 GHz. Theoretical proof is in the following.

Considering only line of sight path existing in ideal anechoic chambers, the transfer matrix neglecting antenna

pattern in free space is a function of frequency as:

$$\boldsymbol{A}(f) = \begin{bmatrix} a_{11}(f) & a_{12}(f) \\ a_{21}(f) & a_{22}(f) \end{bmatrix} = \begin{bmatrix} \frac{1}{4\pi f \tau_{11}} e^{-i2\pi f \tau_{11}} & \frac{1}{4\pi f \tau_{12}} e^{-i2\pi f \tau_{12}} \\ \frac{1}{4\pi f \tau_{21}} e^{-i2\pi f \tau_{21}} & \frac{1}{4\pi f \tau_{22}} e^{-i2\pi f \tau_{22}} \end{bmatrix} \quad (7)$$

Each entry in (7) is as follows:

$$\frac{1}{4\pi f \tau_{ij}} e^{-i2\pi f \tau_{ij}} = \frac{1}{4\pi f_c \tau_{ij}} \frac{f_c}{f} e^{-i2\pi f_c \tau_{ij}} e^{-i2\pi (f-f_c)\tau_{ij}} = a_{ij}(f_c) \frac{f_c}{f} e^{-i2\pi (f-f_c)\tau_{ij}} \quad (8)$$

Substituting (8) into (7), (7) is rewritten as:

$$\boldsymbol{A}(f) = \frac{f_c}{f} \begin{bmatrix} a_{11}(f_c) e^{-i2\pi (f-f_c)\tau_{11}} & a_{12}(f_c) e^{-i2\pi (f-f_c)\tau_{12}} \\ a_{21}(f_c) e^{-i2\pi (f-f_c)\tau_{21}} & a_{22}(f_c) e^{-i2\pi (f-f_c)\tau_{22}} \end{bmatrix} \quad (9)$$

where τ_{ij} denotes the propagation delay from OTA antenna j to DUT antenna i ($i, j \in [1, 2]$). f_c denotes one frequency sample over the frequency band f.

In a specific case that,

$$\tau_{11} = \tau_{12} = \tau_{21} = \tau_{22} = \tau_0 \quad (10)$$

the transfer matrix can be rewritten as:

$$\boldsymbol{A}(f) = \begin{bmatrix} a_{11}(f_c) & a_{12}(f_c) \\ a_{21}(f_c) & a_{22}(f_c) \end{bmatrix} \frac{f_c}{f} e^{-i2\pi (f-f_c)\tau_0} = \boldsymbol{A}(f_c) \frac{f_c}{f} e^{-i2\pi (f-f_c)\tau_0} \quad (11)$$

Thus $\boldsymbol{A}(f)$ is divided into a frequency invariant matrix $\boldsymbol{A}(f_c)$ and a frequency dependent scalar multiplier $\frac{f_c}{f} e^{-i2\pi (f-f_c)\tau_0}$. One calibration matrix $\boldsymbol{G}(f_c)$ is determined for $\boldsymbol{A}(f_c)$ by:

$$\boldsymbol{A}(f_c)\boldsymbol{G}(f_c) = \begin{bmatrix} 1 & 0 \\ 0 & 1 \end{bmatrix} \quad (12)$$

Then isolation levels over the frequency band f using one calibration matrix $\boldsymbol{G}(f_c)$ is calculated according to:

$$\boldsymbol{A}(f)\boldsymbol{G}(f_c) = \boldsymbol{A}(f_c) \frac{f_c}{f} e^{-i2\pi (f-f_c)\tau_0} \boldsymbol{G}(f_c) = \begin{bmatrix} 1 & 0 \\ 0 & 1 \end{bmatrix} \frac{f_c}{f} e^{-i2\pi (f-f_c)\tau_0} \quad (13)$$

Thus good isolation levels are achieved, independent of frequency in the specific case.

However in the normal case that (10) is not satisfied, good isolation levels are achieved provided that (11) can be approximated within a certain frequency range. On condition that the difference among τ_{ij} (depending on the relative location of OTA antennas and DUT antennas) and the frequency separation $f - f_c$ are small, the variation among $(f - f_c)\tau_{ij}$ is negligible so that (9) can be approximate to (11). However, (9) can not be approximate to (11) when the frequency separation $f - f_c$ is large, for the variation among $(f - f_c)\tau_{ij}$ is evident in this situation. Therefore, the isolation levels degradation exists among different component carriers adopting one calibration matrix in anechoic chambers when the frequency separation of component carriers is large.

V. CONCLUSION

The MIMO OTA tesing of CA using RTS method is discussed in this paper where two setups (Setup A and B) are presented to apply the RTS method to CA. The focus is on the establishment of wireless cable connections for CA in the second stage of RTS method. Setup A is to directly use multiple setup resources under the circumstances of single carrier according to the number of component carrier. For each component carrier of CA, the calibration matrix $\boldsymbol{G}_c$ is determined respectively just as it is done in the case of single carrier. Subsequently, the determined $\boldsymbol{G}_c$ is implemented separately for each component carrier in the RF band of CE. In the case that $\boldsymbol{G}_c$ is determined by inverting $\boldsymbol{A}_c$ for each component carrier, the determined $\boldsymbol{G}_c$ is implemented in the digital baseband of CE in Setup B. This setup reduces system cost and calibration time greatly, especially when the number of component carriers is large. Finally, the RTS method for CA is validated in anechoic chambers, and a small RF shielded anechoic box is recommended to save system cost.

ACKNOWLEDGMENT

The authors appreciate the help from Mr. Kristian Bank for practical measurements. They appreciate the valuable comments from Mr. Yilin Ji, Mr. Xuesong Cai, Mr. Yiming Zhang, and Mr. Stanislav Stefanov Zhekov.

REFERENCES

[1] M. A. Jensen and J. W. Wallace, "A review of antennas and propagation for MIMO wireless communications," *IEEE Trans. Antennas Propag.*, vol. 52, no. 11, pp. 2810–2824, Nov. 2004.

[2] G. Yuan, X. Zhang, W. Wang, and Y. Yang, "Carrier aggregation for LTE-advanced mobile communication systems," *IEEE Commun. Mag.*, vol. 48, no. 2, pp. 88–93, Feb. 2010.

[3] Z. Shen, A. Papasakellariou, J. Montojo, D. Gerstenberger, and F. Xu, "Overview of 3GPP LTE-advanced carrier aggregation for 4G wireless communications," *IEEE Commun. Mag.*, vol. 50, no. 2, pp. 122–130, Feb. 2012.

[4] C. Hoymann *et al.*, "LTE release 14 outlook," *IEEE Commun. Mag.*, vol. 54, no. 6, pp. 44–49, Jun. 2016.

[5] M. Jaber, M. A. Imran, R. Tafazolli, and A. Tukmanov, "5G backhaul challenges and emerging research directions: A survey," *IEEE Access*, vol. 4, pp. 1743–1766, Apr. 2016.

[6] E. Chavarria-Reyes, I. F. Akyildiz, and E. Fadel, "Energy-efficient multi-stream carrier aggregation for heterogeneous networks in 5G wireless systems," *IEEE Trans. Wireless Commun.*, vol. 15, no. 11, pp. 7432–7443, Nov. 2016.

[7] M. Iwamura, K. Etemad, M.-H. Fong, R. Nory, and R. Love, "Carrier aggregation framework in 3GPP LTE-advanced," *IEEE Commun. Mag.*, vol. 48, no. 8, pp. 60–67, Aug. 2010.

[8] B. M. Hasiandra and Iskandar, "Planning and performance analysis of downlink inter-band carrier aggregation for LTE-advanced 3GPP released 13," in *Proc. 10th Int. Conf. Telecommun. Syst. Services Appl. (TSSA)*, Oct. 2016, pp. 1–6.

[9] M. Rumney, R. Pirkl, M. H. Landmann, and D. A. Sanchez-Hernandez, "MIMO over-the-air research, development, and testing," *Int. J. Antennas Propag.*, vol. 2012, May 2012, Art. no. 467695, doi: 10.1155/2012/467695.

[10] M. Rumney *et al.*, "Testing 5G: Evolution or revolution?" *Radio Propag. Technol. 5G*, Oct. 2016.

[11] J. T. Toivanen, T. A. Laitinen, V.-M. Kolmonen, and P. Vainikainen, "Reproduction of arbitrary multipath environments in laboratory conditions," *IEEE Trans. Instrum. Meas.*, vol. 60, no. 1, pp. 275–281, Jan. 2011.
[12] P. Kyösti, T. Jämsä, and J.-P. Nuutinen, "Channel modelling for multiprobe over-the-air MIMO testing," *Int. J. Antennas Propag.*, vol. 2012, Mar. 2012, Art. no. 615954, doi: 10.1155/2012/615954.
[13] W. Fan, P. Kyösti, J. Nielsen, and G. F. Pedersen, "Wideband MIMO channel capacity analysis in multiprobe anechoic chamber setups," *IEEE Trans. Veh. Technol.*, vol. 65, no. 5, pp. 2861–2871, May 2016.
[14] A. Khatun *et al.*, "Experimental verification of a plane-wave field synthesis technique for MIMO OTA antenna testing," *IEEE Trans. Antennas Propag.*, vol. 64, no. 7, pp. 3141–3150, Jul. 2016.
[15] W. Fan, P. Kyösti, Y. Ji, L. Hentilä, X. Chen, and G. F. Pedersen, "Experimental evaluation of user influence on test zone size in multi-probe anechoic chamber setups," *IEEE Access*, vol. 5, pp. 18545–18556, 2017.
[16] P.-S. Kildal and K. Rosengren, "Correlation and capacity of MIMO systems and mutual coupling, radiation efficiency, and diversity gain of their antennas: Simulations and measurements in a reverberation chamber," *IEEE Commun. Mag.*, vol. 42, no. 12, pp. 104–112, Dec. 2004.
[17] N. Arsalane, M. Mouhamadou, C. Decroze, D. Carsenat, M. A. Garcia-Fernandez, and T. Monediere, "3GPP channel model emulation with analysis of MIMO-LTE performances in reverberation chamber," *Int. J. Antennas Propag.*, vol. 2012, Jan. 2012, Art. no. 239420, doi: 10.1155/2012/239420.
[18] X. Chen, "Throughput modeling and measurement in an isotropic-scattering reverberation chamber," *IEEE Trans. Antennas Propag.*, vol. 62, no. 4, pp. 2130–2139, Apr. 2014.
[19] R. Mehmood, J. W. Wallace, and M. A. Jensen, "Reconfigurable OTA chamber for MIMO wireless device testing," in *Proc. 10th Eur. Conf. Antennas Propag. (EuCAP)*, Apr. 2016, pp. 1–4.
[20] M. Rumney, H. Kong, and Y. Jing, "Practical active antenna evaluation using the two-stage MIMO OTA measurement method," in *Proc. 8th Eur. Conf. Antennas Propag. (EuCAP)*, 2014, pp. 3500–3503.
[21] W. Yu, Y. Qi, K. Liu, Y. Xu, and J. Fan, "Radiated two-stage method for LTE MIMO user equipment performance evaluation," *IEEE Trans. Electromagn. Compat.*, vol. 56, no. 6, pp. 1691–1696, Dec. 2014.
[22] M. Rumney, H. Kong, Y. Jing, and X. Zhao, "Advances in antenna pattern-based MIMO OTA test methods," in *Proc. 9th Eur. Conf. Antennas Propag. (EuCAP)*, May 2015, pp. 1–5.
[23] *E-UTRA UE Antenna Test Function Definition for Two-Stage MIMO OTA Test Method*, document 3GPP TR 36.978 V13.2.0, Jun. 2017.
[24] Y. Jing, H. Kong, and M. Rumney, "Radiated two-stage MIMO OTA test method progress for antenna performance evaluation," in *Proc. Asia–Pacific Int. Symp. Electromagn. Compat. (APEMC)*, 2016, pp. 729–731.
[25] C. Schirmer, M. Lorenz, W. A. T. Kotterman, R. Perthold, M. H. Landmann, and G. D. Galdo, "MIMO over-the-air testing for electrically large objects in non-anechoic environments," in *Proc. 10th Eur. Conf. Antennas Propag. (EuCAP)*, Apr. 2016, pp. 1–6.
[26] M. Rumney, H. Kong, Y. Jing, Z. Zhang, and P. Shen, "Recent advances in the radiated two-stage MIMO OTA test method and its value for antenna design optimization," in *Proc. 10th Eur. Conf. Antennas Propag. (EuCAP)*, Apr. 2016, pp. 1–5.
[27] Y. Jing, H. Kong, and M. Rumney, "MIMO OTA test for a mobile station performance evaluation," *IEEE Instrum. Meas. Mag.*, vol. 19, no. 3, pp. 43–50, Jun. 2016.
[28] Y. Wang, S. Wu, Z. Yang, P. Shen, and J. Fan, "Studying the effects of location offset on the evaluation of MIMO performance based on the radiated two-stage (RTS) method," in *Proc. IEEE Int. Symp. Electromagn. Compat. (EMCSI)*, Aug. 2017, pp. 464–469.
[29] P. Shen, Y. Qi, J. Fan, and Y. Wang, "The advantages of the RTS method in MIMO OTA measurements," in *Proc. IEEE Int. Symp. Electromagn. Compat. (EMCSI)*, Aug. 2017, pp. 470–473.
[30] W. Fan, P. Kyösti, L. Hentilä, and G. F. Pedersen, "MIMO terminal performance evaluation with a novel wireless cable method," *IEEE Trans. Antennas Propag.*, vol. 65, no. 9, pp. 4803–4814, Sep. 2017.
[31] P. Shen, Y. Qi, W. Yu, and F. Li, "Eliminating RSARP reporting errors in the RTS method for MIMO OTA test," *IEEE Trans. Electromagn. Compat.*, vol. 59, no. 6, pp. 1708–1715, Dec. 2017.
[32] P. Shen, Y. Qi, W. Yu, and F. Li, "Inverse matrix auto-search technique for the RTS MIMO OTA test—Part 1: Theory," *IEEE Trans. Electromagn. Compat.*, vol. 59, no. 6, pp. 1716–1723, Dec. 2017.
[33] W. Fan, P. Kyösti, L. Hentilä, F. Zhang, and G. F. Pedersen, "MIMO device performance testing with the wireless cable method," in *Proc. 12th Eur. Conf. Antennas Propag. (EuCAP)*, Apr. 2018, pp. 1–5.
[34] F. Zhang, W. Fan, X. Wu, and G. F. Pedersen, "Performance testing of MIMO device with the wireless cable method based on particle swarm optimization algorithm," in *Proc. Int. Workshop Antenna Technol. (iWAT)*, 2018, pp. 1–4.
[35] W. Fan, F. Zhang, P. Kyösti, L. Hentilä, and G. F. Pedersen, "Wireless cable method for high-order MIMO terminals based on particle swarm optimization algorithm," *IEEE Trans. Antennas Propag.*, vol. 66, no. 10, pp. 5536–5545, Oct. 2018.
[36] P. Shen, Y. Qi, W. Yu, and F. Li, "Inverse matrix auto-search technique for the RTS MIMO OTA test—Part II: Validations," *IEEE Trans. Electromagn. Compat.*, vol. 60, no. 5, pp. 1288–1295, Oct. 2018.
[37] Y. Ji, W. Fan, G. F. Pedersen, and X. Wu, "On channel emulation methods in multiprobe anechoic chamber setups for over-the-air testing," *IEEE Trans. Veh. Technol.*, vol. 67, no. 8, pp. 6740–6751, Aug. 2018.
[38] P. Liao and M. Mora-Andreu, "LTE carrier aggregation MIMO OTA tests using a reverberation chamber," in *Proc. 9th Eur. Conf. Antennas Propag. (EuCAP)*, May 2015, pp. 1–3.
[39] C. S. P. Lötbäck, A. Skårbratt, and K. Arvidsson, "Over-the-air testing of LTE-advanced features using reverberation chamber," in *Proc. 11th Eur. Conf. Antennas Propag. (EuCAP)*, Mar. 2017, pp. 623–627.
[40] M. Barazzetta, C. Carlini, R. Diamanti, V. M. Primiani, and F. Moglie, "Testing of the carrier aggregation mode for a live LTE base station in reverberation chamber," *IEEE Trans. Veh. Technol.*, vol. 66, no. 4, pp. 3024–3033, Apr. 2017.
[41] Y. Jing, Z. Wen, H. Kong, S. Duffy, and M. Rumney, "Two-stage over the air (OTA) test method for MIMO device performance evaluation," in *Proc. IEEE Int. Symp. Antennas Propag. (APSURSI)*, Jul. 2011, pp. 71–74.
[42] Y. Jing, X. Zhao, H. Kong, S. Duffy, and M. Rumney, "Two-stage over-the-air (OTA) test method for LTE MIMO device performance evaluation," *Int. J. Antennas Propag.*, vol. 2012, May 2012, Art. no. 572419, doi: 10.1155/2012/572419.

HUAQIANG GAO received the B.E. degree in electronic and information engineering from the Harbin University of Science and Technology and the B.A. degree in business english from Heilongjiang University, Harbin, China, in 2016. He is currently pursuing the Ph.D. degree in electronic science and technology with the Beijing University of Posts and Telecommunications, Beijing, China. Since 2018, he has been a Research Intern with the Antennas, Propagation and Millimeter-wave Systems Section, Aalborg University. His research interest includes over the air testing of wireless devices.

WEIMIN WANG received the B.S. degree in communication engineering, the M.S. degree in electronic engineering, and the Ph.D. degree in electronic engineering from the Beijing University of Posts and Telecommunications (BUPT), Beijing, China, in 1999, 2004, and 2014, respectively. In 2014, she joined BUPT. She is currently a Lecturer with the School of Electronic Engineering, BUPT. Her research interests include electromagnetic fields and MIMO OTA measurements.

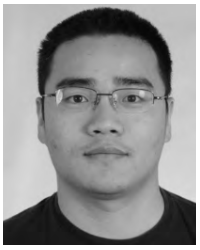

WEI FAN received the B.E. degree from the Harbin Institute of Technology, China, in 2009, the master's degree (Hons.) from the Politecnico di Torino, Italy, the master's degree from the Grenoble Institute of Technology, France, in 2011, and the Ph.D. degree from Aalborg University, Denmark, in 2014. In 2011, he was a Research Intern with Intel Mobile Communications, Denmark. He conducted a three-month internship with Anite Telecoms Oy, Finland, in 2014. He is currently an Associate Professor with the Antennas, Propagation and Millimeter-Wave Systems Section, Aalborg University. His main areas of research are over the air testing of multiple antenna systems, radio channel sounding, modeling, and emulation.

YONGLE WU received the B.Eng. degree in communication engineering and the Ph. D. degree in electronic engineering from the Beijing University of Posts and Telecommunications (BUPT), Beijing, China, in 2006 and 2011, respectively. In 2010, he was a Research Assistant with the City University of Hong Kong, Hong Kong. In 2011, he joined the BUPT. He is currently a Full Professor with the School of Electronic Engineering, BUPT. His research interests include microwave components and wireless systems design.

YUANAN LIU received the B.E., M.Eng., and Ph.D. degrees in electrical engineering from the University of Electronic Science and Technology of China, Chengdu, China, in 1984, 1989, and 1992, respectively. In 1984, he joined the 26th Institute of Electronic Ministry of China to develop the inertia navigating system. In 1992, he held the first post-doctoral position at the EMC Laboratory, Beijing University of Posts and Telecommunications (BUPT), Beijing, China. In 1995, he started holding the second post-doctoral position at the Broadband Mobile Laboratory, Department of System and Computer Engineering, Carleton University, Ottawa, ON, Canada. Since 1997, he has been a Professor with the Wireless Communication Center, College of Telecommunication Engineering, BUPT, Beijing, where he has been involved in the development of next-generation cellular systems, wireless LANs, Bluetooth application for data transmission, EMC design strategies for high-speed digital systems, and EMI and EMS measuring sites with low cost and high performance.

GERT FRØLUND PEDERSEN was born in 1965. He received the B.Sc. degree (Hons.) in electrical engineering from the Dublin Institute of Technology, Dublin, Ireland, in 1991, and the M.Sc. and Ph.D. degrees in electrical engineering from Aalborg University in 1993 and 2003, respectively. He was one of the pioneers in establishing over-the-air (OTA) measurement systems. He has been with Aalborg University since 1993, where he is currently a Full Professor and the Head of the Antenna, Propagation and Networking Laboratory, for 36 researchers. He is also the Head of the Doctoral School on Wireless Communication with some 100 Ph.D. students enrolled. He is also a consultant for the developments of more than 100 antennas for mobile terminals, including the first internal antenna for mobile phones in 1994 with lowest SAR, first internal triple-band antenna in 1998 with low SAR and high TRP and TIS, and lately various multi-antenna systems-rated as the most efficient on the market. He is also involved in joint university and industry projects and received more than U.S. $12 million in direct research funding. He is also the Project Leader of the SAFE Project with a total budget of U.S. $8 million investigating tunable front end including tunable antennas for the future multiband mobile phones. He has published over 175 peer-reviewed papers. He holds 28 patents. His research interests focused on radio communication for mobile terminals, especially small antennas, diversity systems, and propagation and biological effects. The measurement technique is currently well established for mobile terminals with single antennas. He is also deeply involved in MIMO OTA measurements. He was also the Chair of various COST Groups (swg2.2 of COST 259, 273, 2100, and now ICT1004) and a liaison to 3GPP for OTA test of MIMO terminals.